REPORT DOCUMENTATION PAGE

Form Approved
OMB No. 0704-0188

1. AGENCY USE ONLY (Leave blank)	2. REPORT DATE	3. REPORT TYPE AND DATES COVERED
	May 25,1996	Final; 11/25/92- 11/23/95

4. TITLE AND SUBTITLE
Ginga Studies of Black Hole Cadidates:
Multiwavelength Studies Using Temporal Lags and Ginga Archival Studies of QPOs in LMXB Z-Sources

5. FUNDING NUMBERS
G
N00014-93-1-2001

6. AUTHOR(S)
Peter F. Michelson

7. PERFORMING ORGANIZATION NAME(S) AND ADDRESS(ES)
Stanford University
Department of Physics
Stanford, CA 94305

8. PERFORMING ORGANIZATION REPORT NUMBER

9. SPONSORING/MONITORING AGENCY NAME(S) AND ADDRESS(ES)

10. SPONSORING/MONITORING AGENCY REPORT NUMBER

11. SUPPLEMENTARY NOTES

12a. DISTRIBUTION/AVAILABILITY STATEMENT
Approved for public release
Distribution is unlimited

12b. DISTRIBUTION CODE

13. ABSTRACT *(Maximum 200 words)*

The purpose of the research performed under N00014-93-2001 was to carry out analysis of x-ray temporal observations of several bright galactic x-ray binary systems containing neutron stars that are suspected to have weak magnetic fields and rapid spin periods and to study the X-ray timing signals from binaries suspected to contain black holes. Cygnus X-1 is such a source. The observations and analysis were done in a collaborative mode with the Naval Research Laboratory, Washington, D.C. and the Institute of Space and Astronautical Science (ISAS) of Japan. The observations ere performed with the orbiting Japanese x-ray observatory *Ginga*. Analysis was done on computers at Stanford University, NRL and ISAS.

14. SUBJECT TERMS	15. NUMBER OF PAGES
Black holes, X-ray observations, QPOs	35
	16. PRICE CODE

17. SECURITY CLASSIFICATION OF REPORT	18. SECURITY CLASSIFICATION OF THIS PAGE	19. SECURITY CLASSIFICATION OF ABSTRACT	20. LIMITATION OF ABSTRACT
unclssfied	unclassified	unclassified	UL

GENERAL INSTRUCTIONS FOR COMPLETING SF 298

The Report Documentation Page (RDP) is used in announcing and cataloging reports. It is important that this information be consistent with the rest of the report, particularly the cover and title page. Instructions for filling in each block of the form follow. It is important to ***stay within the lines*** to meet ***optical scanning requirements***.

Block 1. Agency Use Only *(Leave blank)*.

Block 2. Report Date. Full publication date including day, month, and year, if available (e.g. 1 Jan 88). Must cite at least the year.

Block 3. Type of Report and Dates Covered. State whether report is interim, final, etc. If applicable, enter inclusive report dates (e.g. 10 Jun 87 - 30 Jun 88).

Block 4. Title and Subtitle. A title is taken from the part of the report that provides the most meaningful and complete information. When a report is prepared in more than one volume, repeat the primary title, add volume number, and include subtitle for the specific volume. On classified documents enter the title classification in parentheses.

Block 5. Funding Numbers. To include contract and grant numbers; may include program element number(s), project number(s), task number(s), and work unit number(s). Use the following labels:

C	- Contract	**PR**	- Project
G	- Grant	**TA**	- Task
PE	- Program Element	**WU**	- Work Unit Accession No.

Block 6. Author(s). Name(s) of person(s) responsible for writing the report, performing the research, or credited with the content of the report. If editor or compiler, this should follow the name(s).

Block 7. Performing Organization Name(s) and Address(es). Self-explanatory.

Block 8. Performing Organization Report Number. Enter the unique alphanumeric report number(s) assigned by the organization performing the report.

Block 9. Sponsoring/Monitoring Agency Name(s) and Address(es). Self-explanatory.

Block 10. Sponsoring/Monitoring Agency Report Number. *(If known)*

Block 11. Supplementary Notes. Enter information not included elsewhere such as: Prepared in cooperation with...; Trans. of...; To be published in.... When a report is revised, include a statement whether the new report supersedes or supplements the older report.

Block 12a. Distribution/Availability Statement. Denotes public availability or limitations. Cite any availability to the public. Enter additional limitations or special markings in all capitals (e.g. NOFORN, REL, ITAR).

- **DOD** - See DoDD 5230.24, "Distribution Statements on Technical Documents."
- **DOE** - See authorities.
- **NASA** - See Handbook NHB 2200.2.
- **NTIS** - Leave blank.

Block 12b. Distribution Code.

- **DOD** - Leave blank.
- **DOE** - Enter DOE distribution categories from the Standard Distribution for Unclassified Scientific and Technical Reports.
- **NASA** - Leave blank.
- **NTIS** - Leave blank.

Block 13. Abstract. Include a brief *(Maximum 200 words)* factual summary of the most significant information contained in the report.

Block 14. Subject Terms. Keywords or phrases identifying major subjects in the report.

Block 15. Number of Pages. Enter the total number of pages.

Block 16. Price Code. Enter appropriate price code *(NTIS only)*.

Blocks 17. - 19. Security Classifications. Self-explanatory. Enter U.S. Security Classification in accordance with U.S. Security Regulations (i.e., UNCLASSIFIED). If form contains classified information, stamp classification on the top and bottom of the page.

Block 20. Limitation of Abstract. This block must be completed to assign a limitation to the abstract. Enter either UL (unlimited) or SAR (same as report). An entry in this block is necessary if the abstract is to be limited. If blank, the abstract is assumed to be unlimited.

*U.S.GPO:1993-0-358-779

Introduction The purpose of the research performed under N00014-93-1-2001 was to carryout analysis of x-ray temporal observations of several bright galactic x-ray binary systems containing neutron stars that are suspected to have weak magnetic fields and rapid spin periods and to study the X-ray timing signals from binaries suspected to contain black holes. Cygnus X-1 is such a source. The observations and analysis were done in a collaborative mode with the Naval Research Laboratory, Washington, D.C. and the Institute of Space and Astronautical Science (ISAS) of Japan. The observations were performed with the orbiting Japanese x-ray observatory *Ginga.* Analysis was done on computers at Stanford University, NRL and ISAS.

The following paper was published with collaborators during the performance period:

Vaughan, B.A., et al. " Searches for millisecond pulsations in low-mass X-ray binaries. II." Ap.J. 435, 362, 1 Nov. 1994

A preprint of a paper entitled "A modified beat frequency modulated accretion model I. Spin periods and magnetic moments of Z-sources inferred from horizontal branch QPO", is about to be submitted for publication.

Inventions and Patents: There were no inventions or patents that resulted from work performed under this contract.

Submitted to the Astrophysical Journal, 1996 RSN

A Modified Beat Frequency Modulated Accretion Model I. Spin Periods and Magnetic Moments of Z-Sources Inferred from Horizontal Branch QPO

Kent S. Wood
Naval Research Laboratory, Washington, D.C. 20375

Peter F. Michelson, Mallory S. E. Roberts
Department of Physics and W.W. Hansen Experimental Physics Laboratory, Stanford University, Stanford, CA 94305

ABSTRACT

We present a modified beat-frequency modulated accretion model appropriate to a description of the horizontal branch oscillations of Z-type low-mass x-ray binaries. This model incorporates several new physical elements: (i) magnetic screening by the accretion disk and neutron star, (ii) radiation pressure dominance in the inner disk, and (iii) stellar rotation effects. Fitted to observational data, the model constrains the surface magnetic field in a typical LMXB Z source to be less than 10^9 G and the stellar spin frequency to be greater than 400 Hz. The predicted high stellar spin frequency falls in a range where observational upper limits on pulsation are not a constraint. The derived magnetic field and spin frequency range are compatible with the fastest radio pulsars.

Subject headings: Z Sources, LMXB, QPO, accretion torques

1. Introduction

Quasiperiodic oscillations (QPO) with intensity dependence (van der Klis et al. 1985) are a common feature in Z-sources. These sources are low mass x-ray binaries (LMXBs) whose x-ray emission evolves through a characteristic sequence of spectral ratios, as observed in a color-color diagram. The three spectral modes comprising the "Z" are known as the horizontal, normal, and flaring branches. In these sources the correlation of QPO frequency with source brightness manifests itself when the source is on the horizontal branch; for this reason the oscillations are also called "horizontal branch oscillations" (HBOs). This effect distinguishes them from other QPO seen when the source is in one of the other spectral states.

A model for HBO has been proposed (Alpar and Shaham 1985) in which the QPO frequency, ν_Q, is the beat frequency of the Kepler orbit frequency, ν_K, at the magnetosphere radius and the neutron star spin frequency, ν_s, i.e.,

$$\nu_Q = \nu_K(R_m) - \nu_s \tag{1}$$

A more detailed model by Lamb et al. (1985) specifies how luminosity oscillations at ν_Q are produced through modulation of the mass transfer rate to the neutron star in a transition zone at the inner disk boundary. The papers cited above lay out the essential features of the beat frequency modulated accretion (BFMA) model.

A fit of parameters from standard magnetosphere models gives a magnetic field $\sim 6 \times 10^9$ G (or magnetic moment $\mu = 6 \times 10^{27}$G cm^3) and a spin frequency $\nu_s \sim 110$ Hz in the case of GX 5-1. Similar values of B and ν_s can be inferred for other sources from QPO data obtained while the source is on the horizontal branch. The magnetospheric modeling concepts used in the BFMA model derive from the model of Ghosh and Lamb (1979; hereafter GL) for accreting binary pulsars. However, the GL magnetospheric model originally pertained to high mass x-ray binaries (HMXB) with large magnetospheres. For LMXBs, it needs modification for effects arising when the magnetosphere radius is near the neutron star surface and radiation pressure modifies the disk structure. In addition, relativistic effects in rapidly-spinning neutron stars that can affect angular momentum transfer in the system need to be considered. There are also technical fine points. For example, in the GL torque theory the fastness parameter, $\omega_s = \nu_s/\nu_K(R_m)$, plays a central role. For a certain critical value of this parameter, ω_{sc}, the accretion torque vanishes. The numerical value of ω_{sc} used in binary pulsar models is not necessarily valid in LMXBs and has even been questioned in high-mass binary pulsars (Wang 1987, Shibazaki 1989). We present here an alternative BFMA model which addresses these problems. Our results suggest that the spin periods in LMXB Z sources are much shorter than previously thought, and the magnetic moments are significantly smaller.

Summaries of the successes of the BFMA model and also of some issues concerning it may be found in Lamb (1989) and van der Klis (1989). The former reference shows how the BFMA models for HBO can be unified with a broader treatment of all behavior of Z-type LMXB sources. The latter reference is a more comprehensive review of QPO observations. The BFMA successfully fits the intensity dependence of the HBO. The transition zone modulation picture accounts for the correlation of the QPO intensity with low-frequency noise (LFN), although there remains an unresolved issue concerning how this correlation extends to the shortest timescales (Norris et al. 1990, Mitsuda et al. 1991). The reader is also referred to Lewin, Van Paradijs & Van der Klis (1988) for a review of QPO observations in a number of sources and a description of other models of the QPO phenomena.

A major success for the beat frequency model is an observation of a QPO in the transient source EXO 2030+375 (Angelini, Stella and Parmar 1989) which conforms phenomenologically to the beat frequency model with parameters re-scaled into a different range of ν_s and B appropriate to accreting binary pulsars. Because this source is detected as a pulsar, the spin period is a known quantity in this case and not a free parameter to be fitted to observations such as variation of QPO frequency with intensity. This case argues persuasively that intensity modulation at the beat frequency between $\nu_K(R_m)$ and ν_s is a reality in some neutron star binary systems. Validation of the standard BFMA model is less complete in the LMXB systems for which it was first proposed. Indeed there are significant problems with it in that context. Most conspicuously, careful searches have not detected coherent x-ray pulsations in those systems (Wood et al. 1991, Hertz et al. 1990, Vaughan et al. 1994). Upper limits on coherent modulation near or below 1 percent have been established for spin frequencies up to 500 Hz in all 6 of the Z-type sources (see Table 1). Our goal is to achieve a satisfactory match of the BFMA picture to observations of HBO in LMXBs.

An additional motivation to re-examine the estimated spin frequencies of these systems is the possibility of an evolutionary link from low-mass x-ray binary systems to radio millisecond pulsars (Helfand, Ruderman & Shaham 1983, Joss & Rappaport 1983, Paczynski 1983, Savonije 1983). The fastest of the millisecond pulsars have spin periods near 1.6 ms and magnetic fields as low as 10^8 G (Camilo, Thorsett & Kulkarni 1994), values significantly lower than those obtained by conventional BFMA model fits to HBO. We will explore whether such radio pulsars are compatible with our modified BFMA picture.

The spin period of LMXB neutron stars is a central issue. Therefore, we start with a more complete discussion of the interpretation of upper limits obtained from period searches. Subsequent sections present the modified BFMA model, apply it to HBO observations, discuss alternative ways to treat details, and finally return to further observational issues

and tests.

2. Interpretation of Upper Limits on Pulsation

Wood et al. (1991) summarize why LMXB spin periods should lie in the millisecond range. The case for this conclusion was persuasive even before QPO were discovered. The picture of disk accretion with at most a weak magnetic field requires eventual spin-up to high frequency. Accreting material continually adds angular momentum to the star, except perhaps near breakup (Popham & Narayan 1991). Detection of HBO in a source makes the case even stronger if the BFMA model is accepted. However, sensitive searches for spin periods in several LMXB QPO sources have not detected coherent modulation down to the 1% level in pulsed amplitude (Vaughan et al. 1994).

The interpretation of limits on pulsations in Z sources has been presented in several earlier papers, primarily in the context of determining whether limits for spin frequencies near 100 Hz were consistent with the standard BFMA model or possibly constituted a basis for rejecting that model. We now re-examine the issue from a different standpoint, taking the BFMA picture as provisionally correct and asking instead what is the most reasonable value for the spin frequency. We describe several new points not covered in the older discussions.

Pulsation upper limits have been growing more stringent with refinements in search technique and improvements in data. When the BFMA was first proposed the upper limits for some Z sources were near 10%. More recent upper limits reach levels of a few times 10^{-3} out to frequencies approaching 500 Hz (see Table 1), which is the Nyquist frequency for observations conducted with the Ginga satellite (Wood et al. 1991,Vaughan et al. 1994). At higher spin frequencies it also becomes progressively more expensive computationally to overcome smearing of the Fourier power spectrum due to the unknown orbital acceleration, which makes searching trial grids of acceleration parameters a necessity.

Several mechanisms have been proposed to account for the non-detections of spin periods. Since a magnetic field and channeling of flow near the star are central to the BFMA picture it is difficult to avoid uneven heating of the surface that results in production of emission modulated at the spin frequency. The mechanisms proposed to reduce this pulsation below observable levels include (i) gravitational lensing and, (ii) scattering in a hot cloud or corona surrounding the star. We review each of these in turn.

Gravitational lensing. Wood et al. (1988) calculated the effects of lensing, exploring variation of polar cap sizes, surface gravity, and geometry of the observer and field axis.

Two antipodal caps were used, a choice consistent with a dipole field and one that minimizes resulting pulsation. A neutron star with a radius of 2 R_s (8.3 km for $1.4M_\odot$) can reduce pulsation to about 7×10^{-3} relative amplitude modulation for a 45° misalignment between the dipole field axis and the observer's line-of-sight. Such a small radius is consistent with only the softest of the proposed equations of state for neutron star matter (Friedman, Ipser & Parker 1986). If the stellar radius is increased to $2.5R_s$ (10.4 km) then the pulse amplitude is reduced only to about 1.4%.

These numbers are consistent with the limits available in 1987 but more recent limits reach lower values, hence the lensing explanation is becoming marginal even for slowly rotating stars. A further problem has been raised by Chen and Shaham (1989), who have studied effects of extremely high surface velocity (rapid rotation). Most of their analysis pertains to very high velocities, such as would be found near spin periods of 1 millisecond. Special relativistic beaming effects and redshifting from the emission frame to the observer's frame acting on realistic emission spectra can overcome the gravitational lensing effects and enhance pulsation. The difficulty in applying these results to neutron stars with parameters implied by the standard BFMA model is that the surface velocities are very small compared with those used in the calculations, only 0.02 c at the surface of a star with radius 10 km and a spin period of 10 ms. The effects increase roughly as the surface velocity.

The primary uncertainty in evaluating the effects of gravitational lensing on pulse supression comes from our ignorance of the quantity M/R for neutron stars. Available theoretical models of neutron stars are not very constraining and observational evidence is also inconclusive. If future observational results should settle this point in favor of stellar radii greater than about 9 km (for $1.4M_\odot$) then gravitational lensing as an explanation for the lack of detectable coherent pulsations will be excluded, leaving only the explanations that follow.

Coronal scattering. Bussard et al. (1988) investigated the effects of a hot, spherical scattering cloud on QPO behavior. They found that power spectra intrinsic to the source can be severely attenuated at high frequencies by scattering in a hot coronal cloud with the amount of attenuation depending on optical depth and cloud radius. The intrinsic power spectra can be related to the observed spectra by a simple frequency-dependent transmission function $T(\nu) = P_{obs}/P_{initial}$ of the form

$$T(\nu) = e^{-2\tau}[1 + (e^{2\tau} - 1)\gamma_\alpha^2/(\gamma_\alpha^2 + 4\pi^2\nu^2)] \qquad (2)$$

At high frequencies, $\nu > (\gamma_\alpha/2\pi)e^\tau$, this function asymptotically approaches $e^{-2\tau}$, where τ is the Thompson optical depth. At lower frequencies the transmission function has a roughly Lorentzian shape, falling off as ν^{-2} above a frequency corresponding to $\gamma_\alpha/2\pi$, where γ_α is approximately given by the inverse of the product of the optical depth of the

cloud and its light-crossing time. Early spectral fittings (White & Holt 1982, Shibazaki & Mitsuda 1984, , Hirano et al. 1984,) suggested a hot cloud with optical depth ranging from less than 1 to a few. More recent fittings of Exosat data for 4 Z-sources estimate optical depths in the range 4-7 (Schulz & Wijers 1993). Observed temporal lags in the QPO source Cygnus X-2 (Hasinger 1986, Mitsuda & Dotani 1989), if due primarily to scattering, suggest a cloud radius greater than 1000 km (Bussard et al. 1988).

As pointed out by Bussard et al., their results strictly apply only to an isotropically emitting source which pulses in time. Coherent pulsations from a QPO source would likely arise due to beaming from the surface of a rapidly-spinning neutron star in which case both isotropization of the beam due to angular diffusion and smearing due to variations in photon residence time in the cloud must be considered. Brainerd and Lamb (1987) treated the former effect. However if the stellar rotation period is sufficiently short compared to the diffusion time, $\tau R_c/c \sim \gamma_\alpha^{-1}$, then radial diffusion will be the most important effect and the Bussard et al. results can be used to estimate the attenuation of coherent pulsations (as well as QPO oscillations) by the cloud.

In the standard BFMA model (Alpar and Shaham 1985, Lamb et al. 1985), the neutron star rotation frequencies are estimated to be just above 100 Hz and the QPO frequency ranges from 5 to as high as 50 Hz. As shown by Bussard et al. (1988), if we require that the power at the QPO frequency be relatively undiminished while power above 100 Hz be strongly attenuated, the radius of the scattering cloud is constrained. That is $\nu_Q \leq (\gamma_\alpha/2\pi)$. For $\tau = 5$ this implies $R_c \leq 550$ km. At frequencies above $(\gamma_\alpha/2\pi)$ the power attenuation is approximately $(\gamma_\alpha/2\pi)^2/\nu^2$ until it reaches a limiting value of $e^{-2\tau}$ at high frequencies. Thus if $\nu_{Qmax} \sim 50$ Hz, then the coherent pulse amplitude is reduced to 0.50 its original value for $\nu_s = 100$ Hz and 0.08 for $\nu_s = 640$ Hz.

In Figure 1 we compare the pulsational upper limits for LMXB sources with the attenuation expected from coronal scattering and from gravitational lensing. The viability of either of these modulation supression mechanisms is beginning to be severely strained by the observed upper limits for frequencies below approximately 500 Hz. It may be that the simplest explanation for the lack of detection of spin periods in LMXB sources is that the spin periods are less than 2 ms. In the remainder of this paper we explore the viability of this hypothesis. Ultimately, however, the issue will be resolved observationally.

3. Magnetosphere Model

The relationship giving the magnetosphere radius in terms of the mass accretion rate $\dot{M}$ and the stellar magnetic moment μ in the conventional BFMA model is

$$R_m = 0.52 R_A = 34\mathrm{km}\left(\frac{\mu_{27}^2}{\dot{M}_{17} m^{1/2}}\right)^{2/7}, \tag{3}$$

where μ_{27} and $\dot{M}_{17}$ are the stellar magnetic moment and mass accretion rate, respectively, in units of 10^{27}G cm^3 and 10^{17}gm s^{-1}. m is the neutron star's mass in units of $1M_\odot$, and R_A is the spherical Alfvén radius.

Although there is minor disagreement as to the value of the numerical prefactor, most authors assume this dependence (Alpar and Shaham 1985, van den Heuvel 1977, Lamb et al. 1985). The relation was applied by GL to magnetically-coupled accretion torques acting on x-ray pulsars in binary systems. Magnetic moments in those cases are typically much larger than 10^{29}G cm^3. Spin periods are on the order of the Kepler period at R_m; seconds to hundreds of seconds. In LMXB systems magnetic moments are weaker by 10^{3-4}. This causes the magnetosphere to be far smaller, hence new physical conditions and considerations arise.

The resemblance of HBOs in LMXBs to the one seen in the HMXB binary pulsar EXO2030+375 shows it is reasonable to attempt to extend these ideas to the smaller LMXB magnetospheres. That is the framework for our model, i.e., we assume that a disk, a magnetosphere, and a relatively narrow disk-magnetosphere transition zone continue to exist in the LMXB case. However, at least three factors cause assumptions carried forward from the HMXB disk-magnetosphere picture to become questionable in this limit. (i) Spin frequencies become very high (i.e. ν_s approaches $\nu_K(R_m)$) and can even approach the breakup or mass-shedding limit. (ii) Because the disk likely comes within a few stellar radii of the neutron star's surface, magnetic screening can distort the field configuration substantially from a dipole. (iii) When the accretion luminosity L_x approaches the Eddington limit the accretion disk just outside the magnetosphere is likely dominated by radiation pressure, ultimately becoming unstable when the luminosity approaches very close to or exceeds L_{Edd}. However, our working hypothesis is that for LMXB Z sources on the HB the luminosity is low enough that the required revision is an incorporation of radiation pressure into the disk-magnetosphere model and not some more radical recourse.

Some of these needs for revision have been noted in earlier work. For example, White and Stella (1988) have offered prescriptions for including radiation pressure in the determination of the magnetosphere radius within the context of the model of GL. They consider a number of different models and argue that none can be excluded as models for

at least some of the observed QPOs. However, not all these models are workable for HBO because not all give intensity dependence, to say nothing of the other phenomenology.

Aside from the revisions to the conventional picture of the disk-magnetosphere interaction that are necessary for bright LMXB sources, there are other, more generic, deficiencies in the conventional magnetosphere models. For example, Wang (1987) has pointed out an inconsistency in the treatment of the magnetic pitch angle in the disk in the original Ghosh-Lamb model. Wang's revision of the GL model leads to a substantially larger value of the critical fastness parameter ω_{sc}, primarily because Wang predicts a smaller value for the pitch angle in the outer disk and therefore a smaller spin-down contribution to the total accretion torque on the star. If the QPOs observed in HMXB sources are due to the beat frequency mechanism, then the fastness parameters derived from the observations are in reasonable agreement with Wang's model applied to gas pressure dominated disk accretion (see discussion in Appendix). However, Wang's model does not have a narrow transition zone between Keplerian flow in the disk and the approximately co-rotating magnetosphere. This zone is a feature of the Ghosh-Lamb model and appears to be a necessary feature if the beat frequency model of QPO is correct.

There are a number of other problems with any of the conventional disk-magnetosphere models. Given the theoretical difficulties of the problem and the present state of observations, a compelling theory that is applicable to LMXBs is not likely to be available soon. Nonetheless, it is possible to make progress on the spin period-QPO dilemma in LMXBs by the following approach: (i) we introduce a set of modifications to the standard treatment of disk-magnetosphere interactions to deal with known deficiencies; (ii) we parameterize these modifications and combine them into a "modified BFMA model", and (iii) we explore this parametrized model over a range of the parameters that we believe is reasonable, to see how various modifications constrain the spin frequency and magnetic moment of neutron stars in Z sources. This is done by requiring agreement of eq.(1) with the intensity-dependent QPO frequency observed on the horizontal branch. Anticipating the conclusion, we find that over a substantial part of the plausible range of the parameters of the model, the spin frequencies inferred are much larger than those implied by the conventional model and that the neutron star magnetic moments required are about the same as those of the fastest millisecond radio pulsars. Additionally, the new model offers some insights into issues regarding the QPO shot rate and the correlation of QPO power and low frequency noise (LFN) power raised by Ginga observations (Norris et al. 1990, Mitsuda et al. 1991). While we believe these modifications are physically well-motivated, it should be noted that at this time it is virtually impossible to directly establish the validity of this modified model.

The details of the modifications to the disk-magnetosphere interaction picture are presented in the remaining subsections. Here we only summarize these modifications and the associated parameters. The reader not interested in the details can skip to section 4. The areas of modification and the associated parameters are:

(i) *Angular Momentum Transfer:* Throughout the remainder of this section the disk is modeled with radiation pressure as the dominant pressure in the inner regions, according to the prescription summarized by Treves et al. (1988). Torques at the magnetosphere boundary are modeled keeping terms of order δ/R_m, where δ is the width of the transition zone. Vertical mass loss from the transition zone, associated with material transfered onto closed field lines, is explicitly taken into account with a parameter β_m, which is unity when there is no vertical loss.

(ii) *the magnetic pitch:* We consider the original model of GL in which the magnetic pitch angle $\gamma_\phi = B_\phi/B_z$ in the narrow transition zone is of order unity. We also consider the model of Wang (1987) in which the pitch angle depends on physical parameters of the disk and the star. We parameterize γ_ϕ in our model by $\gamma_\phi = (\gamma_w)^{\beta_\gamma}$, where $0 \leq \beta_\gamma \leq 1$ and γ_w is Wang's expression for the pitch angle given by eq. (8) below.

(iii) *width of transition layer:* We essentially follow the Ghosh-Lamb treatment. An important parameter in determining the width of the transition zone is the average radial velocity v_r through the transition zone. GL take v_r to be the free-fall velocity v_{ff}, given by eq. (14) below. However, when the fastness parameter approaches unity, v_r may be better approximated by the radial drift velocity in the disk v_d just outside the transition zone. v_d depends on the viscosity of the disk. In order to explore a range of models between these limits we parametrize the radial velocity as $v_r = (v_{ff})^{1-\beta_v}(v_d)^{\beta_v}$, where $0 \leq \beta_v \leq 1$.

(iv) *effective magnetic moment:* We model the bare stellar magnetic field as a dipole with moment μ. As originally noted by GL, screening currents in the disk and the diamagnetic behavior of the neutron star will lead to an enhancement of the field in the magnetosphere. While this is probably negligible for x-ray pulsars, in the case of LMXBs, where μ is likely to be several orders of magnitude smaller and the disk extends to within a few stellar radii of the surface, the enhancement effect is more important. We model this enhancement in terms of an effective dipole moment $\mu_{eff}(r)$. A parameter of importance that appears later is $\Lambda_\mu = -(R_m/\mu_{eff})d\mu_{eff}/dR_m$.

3.1. Angular Momentum Transfer

Following the approach of GL, we derive an expression for the magnetosphere radius that explicitly includes the effects of stellar rotation. We assume that the Keplerian flow of the disk ends at the radius where the magnetic coupling to the disk is large enough to remove sufficient angular momentum from the flow to enforce co-rotation. The relevant equation of angular momentum conservation is

$$\frac{d(\dot{M}r^2\Omega(r))}{dr} = r^2\Omega\frac{d\dot{M}}{dr} + \frac{B_\phi}{B_z}r^2 + \text{viscous stresses.} \tag{4}$$

Next, we assume that the transition from nearly Keplerian flow in the disk to co-rotation occurs in a narrow transition boundary layer of width $\delta << r$. Ignoring viscous stresses (since magnetic stress >> viscous stress in the transition layer), we have, after integrating and keeping terms to first order in δ/R_m,

$$\dot{M}R_m^2\Omega_K(R_m)[(1-\omega_s) + \frac{1}{2}\delta/R_m] \sim< \gamma_\phi > B_z^2R_m^3(\delta/R_m) + \int_{R_m}^{R_m+\delta} r^2\Omega(d\dot{M}/dr)dr \tag{5}$$

where $< \gamma_\phi >=< B_\phi/B_z >$ is the average magnetic pitch angle in the boundary layer transition zone and $\omega_s = \Omega_s/\Omega_K(R_m)$. GL show that δ is approximately equal to the electromagnetic screening length. We will not make this assumption unless explicitly noted. Except for the second term on the left hand side and the mass loss term on the right hand side, eq.(5) is identical to eq.(43) of GL.

Now consider the mass loss term. GL treat mass flow out of the disk, for example by vertical mass flow, in a very approximate manner by introducing a "gate function" $g(r)$ such that $d\dot{M}/dr = 4\pi\rho c_s g(r)$, with $g(r) = 0$ at and outside the outer edge of the boundary layer and $g(r) = 1$ well inside the boundary layer. c_s and ρ are the sound speed and density, respectively. For simplicity we will account for vertical mass flow out of the disk by introducing a parameter β_m such that the radial mass flow rate $\dot{M}_r(r) = (1-\beta_m)[r-R_m]\dot{M}/\delta + \beta_m\dot{M}$ in the transition boundary layer. In this case $\dot{M}$ is the radial mass flow rate in the disk well outside the transition layer. For $\beta_m = 0$, there is no radial mass flow through $r = R_m$, while for $\beta_m = 1$ there is no vertical mass loss. Evaluating the mass-loss term in eq.(5) in this manner results in

$$\dot{M}R_m^2\Omega_K(R_m)[\tilde{\beta}_m(1-\omega_s) + \frac{1}{2}\delta/R_m] \sim< \gamma_\phi > B_z^2R_m^3(\delta/R_m) \tag{6}$$

where $0 \leq \beta_m \leq 1$ and $\tilde{\beta}_m = (2\beta_m + 1)/3$. Scaling to numerical values appropriate to QPO sources, and assuming $B_z = \mu/r^3$, eq.(6) gives

$$R_m = 68.8\text{km}\left(\frac{\mu_{27}^2(\delta/R_m) < \gamma_\phi >}{m^{1/2}\dot{M}_{17}[\tilde{\beta}_m(1-\omega_s) + \frac{1}{2}\delta/R_m]}\right)^{2/7} \tag{7}$$

If $\tilde{\beta}_m(1-\omega_s) << \frac{1}{2}\delta/R_m$ then R_m does not explicitly depend on the form of δ/R_m. In this limit the criterion for determining R_m is the same as that given by Wang (1987). GL did not include the second term on the left hand side of eq. (6). For values of ω_s near the critical value in the GL theory this term is negligible anyway. However, using the magnetic pitch expression of Wang to evaluate the accretion torque (see Appendix) gives critical values of ω_s much closer to unity. In this case the two terms on the left of eq. (6) can be of the same magnitude.

3.2. The Magnetic Pitch

To proceed further we must specify $< \gamma_\phi >$ and δ/R_m. First consider the magnetic pitch. Following Wang (1987), we assume that the azimuthal component of magnetic field is generated as a result of the relative rotation between the magnetosphere and the disk and is limited by either annihilation of toroidal flux near the midplane of the disk or by expulsion of flux through the effects of magnetic buoyancy (Parker 1955). Setting the loss rate equal to the rate of generation gives

$$\gamma_\phi = B_\phi/B_z \sim (\lambda/\zeta)^{1/2}[(\Omega_K(r) - \Omega_s)h/v_{Az}]^{1/2} \tag{8}$$

where $v_{Az} = B_z/(4\pi\rho)^{1/2}$ is the associated Alfvén velocity. (λ/ζ) is a dimensionless parameter expected to be greater than or the order of unity. h is the half-height of the disk. Assuming $\dot{M} = 4\pi\rho r v_r h$ in the disk and averaging over the transition zone, eq.(8) gives

$$< \gamma_\phi >= (\lambda/\zeta)^{1/2}[(\dot{M}/R_m)(h/R_m)(v_K/v_r)\Omega_K]^{1/4}[(1-\omega_s)/B_z]^{1/2} \equiv \gamma_w \tag{9}$$

where v_r is the average radial flow velocity in the transition zone. In the original treatment of GL, $< \gamma_\phi >$ was taken to be a constant of order unity in the transition zone. Also, to calculate the aximuthal magnetic field pitch in the outer disk caused by interaction of the magnetosphere with the Keplerian flow of the disk, GL estimated the size of B_ϕ by estimating its rate of amplification by differential rotation as $\lambda|\Omega_K - \Omega_s|B_\phi$, where λ is a numerical factor of order unity. As pointed out by Wang (1987) and Ghosh and Lamb (1991), the induction equation actually implies that B_ϕ is generated at the rate $\lambda|\Omega_K - \Omega_s|B_z$. This expression leads to eq. (8), which generally gives smaller values of the magnetic pitch in the outer transition zone as compared with GL and thus gives smaller values of the spin-down contribution to the torque and therefore larger values of the critical fastness parameter. In any case γ_ϕ is likely limited to values $\sim 1-3$ by the expansion of the magnetosphere that occurs when the magnetospheric magnetic field is strongly sheared (Ghosh & Lamb 1991). From the numerical estimate given below we find that $< \gamma_\phi >$ given by eq.(9), for parameters appropriate to LMXB Z sources, is probably below this range of limiting values.

3.3. Width of Transition Layer

In the GL theory δ is equal to the electromagnetic screening length given by

$$\delta = \frac{(c^2/4\pi)}{(v_r \sigma_{eff})} \tag{10}$$

where v_r is the average radial plasma velocity in the transition layer and σ_{eff} is the effective disk conductivity for poloidal currents;

$$\sigma_{eff} = \frac{c^2}{4\pi}\frac{1}{hr}\frac{\gamma_\phi}{(\Omega(r) - \Omega_s)} \tag{11}$$

Combining eq.(10) and (11) gives

$$\delta/r = \frac{1}{< \gamma_\phi >}\left(\frac{v_K}{v_r}\right)\left(\frac{h}{r}\right)(1 - \omega_s) \tag{12}$$

Substitution of this expression into into eq.(7) gives

$$R_m = 68.8\mathrm{km}\left(\frac{\mu_{27}^2 (v_K/v_r)(h/R_m)}{m^{1/2}\dot{M}_{17}[\tilde{\beta}_m + \frac{1}{2}(1/ < \gamma_\phi >)(v_K/v_r)(h/R_m)]}\right)^{2/7} \tag{13}$$

In their treatment GL set $< \gamma_\phi > \approx 1$ and approximate v_r by the free-fall velocity through the transition layer;

$$v_r \sim (\delta/r)^{1/2} v_K (1 - \omega_s^2)^{1/2} = v_{ff} \tag{14}$$

In this limit, eq.(12) and (14) give [see also White and Stella (1988) and GL (1979)]

$$(\delta/r)_{GL} = (h/r)^{2/3}(1 - \omega_s)^{1/3}(1 + \omega_s)^{-1/3} \tag{15}$$

While eq.(14) is an appropriate estimate when $\omega_s << 1$, as $\omega_s \to 1$, the characteristic radial velocity in the transition layer may be better approximated by the radial drift velocity in the disk v_d just outside the transition layer. v_d is determined primarily by the viscosity of the disk. For a radiation pressure dominated disk (RPD), in the α-disk approximation, (Treves, Maraschi & Abramowicz 1988)

$$(v_K/v_d)(h/r) = (1.4/\alpha c)(2GM/c^2)^{-3/2}(GM)^{1/2} r \tag{16}$$

For a RPD disk, the condition that the radial velocity exceed the free-fall value is $(1 - \omega_s) << 0.09\alpha^{3/2}(\dot{M}/\dot{M}_{edd})(M/1.5M_\odot)^{5/2}(R_m/22.5\mathrm{km})^{-5/2}$. Since we expect $(1 - \omega_s) \approx 0.04 - 0.06$ (see below), the appropriate limiting value for v_r depends on the

viscosity parameter α. We will consider this further below. Assuming for the moment that $v_r = v_d$ and conditions appropriate to LMXB Z-sources ($B_z \leq 10^9 G(R_s/r)^3$ and $(1-\omega_s) \approx 0.06$), we find $< \gamma_\phi > \sim 0.1\alpha^{-1/4}(B_z/10^9 G)^{-1/2}(\dot{M}/10^{18}\mathrm{gm\ s^{-1}})^{1/4}$. Thus it is likely that the average magnetic pitch in the transition zone does not exceed unity.

Our use of equations describing a RPD disk implicitly carries the assumption that instabilities do not destroy the disk altogether. There is good reason to think that this is the case when HBO are present, because the constancy of the QPO and its gradual, repeatable variation with changing luminosity suggest a degree of constancy associated with the disk structure. It is also possible that instabilities associated with RPD disks may lead to clumps in the accretion flow which are a necessary ingredient of the beat frequency model, since if there is no azimuthal variation of density in the transition zone then the QPO will be absent.

In the limit where the transition zone velocity is the free-fall value, eq.(13) gives the result that would have been obtained by combining the GL prescription for R_m and δ/R_m with the RPD disk prescription for h/R_m. However, eqn.(13) is more general than this. In order to explore a range of viable magnetospheric models and guided by the above considerations about v_r and $< \gamma_\phi >$, we adopt the following parameterizations;

$$< \gamma_\phi >= (\gamma_w)^{\beta_\gamma}\ , v_r = (v_{ff})^{1-\beta_v}(v_d)^{\beta_v} \tag{17}$$

where γ_w is given by eq.(9).

The plausible range for the exponents β_γ and β_v is $0 \leq \beta_\gamma \leq 1$ and $0 \leq \beta_v \leq 1$. The GL values are obtained for $\beta_\gamma = 0$ and $\beta_v = 0$, while the Wang values are obtained for $\beta_\gamma = 1$ and $\beta_v = 1$. Eqs. (9), (12), (14), (15), (16) and (17) provide a consistent set of equations for determining R_m in the limit of a RPD disk once $B_z(r)$ is specified. We assume that $B_z(r) = \mu_{eff}/r^3$, where $\mu_{eff}(r)$ is an effective magnetic dipole moment that includes corrections due to screening currents in the disk.

At this point we can derive a relationship between the spin frequency and the effective magnetic dipole moment, utilizing the observational constraint of the beat frequency model implied by Eq. (1).

$$\mu^2_{eff27}(R_m) = 4.8 \times 10^4 \frac{m^{5/3}\dot{M}_{17}}{(\nu_s + \nu_Q)^{7/3}}\left[\frac{\tilde{\beta}_m v_d^{\beta_v} v_{ff}^{1-\beta_v}}{2\pi h(\nu_s + \nu_Q)} + \frac{1}{2\gamma_w^{\beta_\gamma}}\right] \tag{18}$$

where $\dot{M}_{17}$ is the radial mass flow outside the transition region in units of $10^{17}\mathrm{gm\ s^{-1}}$.

3.4. Effective Magnetic Moment

The final major ingredient in our model is a treatment of the modification in magnetic field structure caused by the (partial) exclusion of magnetic flux from the disk and the diamagnetic behavior of the neutron star. The main effect is an enhancement of the magnetic field in the magnetosphere. This is represented by an effective magnetic moment:

$$\mu_{eff}(r) = \mu[R_m/(R_m - R_s)]F \tag{19}$$

where R_s is the equatorial radius of the neutron star. μ is the magnetic moment of the star in the absence of the disk. F is a correction factor of order unity that characterizes what fraction of the field lines between R_m and the light cylinder are excluded from the disk. It will be taken to be unity here. Equation (19) is the simplest functional form for μ_{eff} that has the correct behavior for large R_m (i.e. $\mu_{eff} \rightarrow \mu$) and also conserves magnetic flux (when $F = 1$). Equation (19) as given above does not include allowance for any quadrupole terms in the magnetic field of the bare star that may become appreciable within a few tens of kilometers of the surface. Such a quadrupole term can increase the ratio μ_{eff}/μ to a larger value than that given by (19).

3.5. Equilibrium Spin Period Constraint

The prescription for the magnetic pitch angle given by eq.(8) has important consequences for the accretion torque and the equilibrium stellar spin frequency. Wang (1987) showed that for a gas-pressure dominated disk the accretion torque vanished for a critical value of the fastness parameter $\omega_{sc} = 0.94$ (compared with 0.35 in the original GL theory). More recently, Wang (1995) found for various physically plausible estimates of the dissipation timescale τ, that $\omega_{sc} = 0.875 - 0.950$. A similar calculation (See Appendix) can be done for a radiation pressure dominated disk, with the result that $\omega_{sc} \simeq 0.918$. This result should be regarded as a lower limit since in a system containing a rapidly-spinning neutron star the spin-down contribution to the torque is likely cutoff near the light-cylinder radius in the disk, R_{lc}. In a typical LMXB Z source, $R_{lc} = c/\Omega_s$ may only be a few times larger than the magnetosphere radius. As a result ω_{sc} could be as large as 0.978.

Within the context of the BFMA model, the stellar spin frequency can be expressed as

$$\nu_s = \nu_Q \omega_s/(1 - \omega_s) \tag{20}$$

For the LMXB Z sources, such as GX5-1, we do not know the location along the Z diagram where the accretion torque is zero. If we assume that the torque is zero somewhere along the

normal branch, then the highest observed HB QPO frequency, along with the theoretical lower limit on ω_{sc} discussed above (ie., 0.918), places a lower limit on ν_s. For GX5-1, ν_Q as high as 36 Hz has been observed on the HB. This implies $\nu_s \geq 400 Hz$.

4. Comparison With QPO Observations

To use the above magnetospheric model to fit HBO oscillations, it is convenient to assume the form

$$\nu_Q = a(L_x)^{\xi} - \nu_s \tag{21}$$

with

$$L_x = \Phi_{grav} \dot{M}_{acc} \tag{22}$$

Φ_{grav} is the gravitational potential at the surface of the neutron star and the exponent ξ is related to the logarithmic derivative of R_m with respect to $\dot{M}$ by

$$\xi = -\frac{3}{2}\frac{\partial log R_m}{\partial log \dot{M}} \tag{23}$$

$\dot{M}_{acc}$ is the amount of mass flow which ultimately gets accreted onto the neutron star. In our model, this is related to $\dot{M}$ and β_m. If $\beta_m = 1$ then there is no vertical mass loss and $\dot{M}_{acc} = \dot{M}$. If the corotation radius is outside the transition region, i.e. $R_c > R_m + \delta$ then the mass flowing vertically out of the disk is trapped by the magnetic field and is eventually channeled onto the neutron star, and $\dot{M}_{acc} = \dot{M}$ still holds. If $R_m < R_c < R_m + \delta$, then the vertical mass flow outside the corotation radius is ejected from the system by the propellor mechanism (). In this case $\dot{M}_{acc} = [(1 - \beta_m)(\omega_s^{-2/3} - 1)R_m/\delta + \beta_m]\dot{M}$. In many cases, simply letting $\dot{M}_{acc} = \dot{M}$ is sufficient. However, as $\omega_s \rightarrow 1$, letting $\dot{M}_{acc} = \beta_m \dot{M}$ may be a better approximation.

Some authors at this point introduce an additional parameter β_L such that L_x varies as $\dot{M}^{\beta_L}$. For simplicity, we refrain from introducing such a parameter. It proves unnecessary for obtaining satisfactory agreement with observation.

In applying this form to HBO data it is worthwhile to recognize that there is an essentially inverse relationship between ν_s and ξ. This can be seen in a simple way if we assume that the fit is constrained to pass through a pair of points on the curve $\nu_Q = \nu_Q(L_x)$. Call these two points $(\nu_{Q,i}, L_{x,i})$, $i = 1, 2$. These could be taken to be representative points near ends of the curve. Then

$$\nu_s = \nu_{Q,1}\left(\frac{(\chi_\nu - 1)}{(\chi_L^{\xi} - 1)} - 1\right), \tag{24}$$

where $\chi_L = L_{x,2}/L_{x,1}$ and $\chi_\nu = \nu_{Q,2}/\nu_{Q,1}$. ν_s is completely determined by two data points and ξ. Given ξ, the allowed range of ν_s for a source is determined by the error propagation in the above equation. Note that the calibration of the luminosity does not enter into determination of ν_s; only the ratio χ_L affects the result. Since relative uncertainties in the numerical values of the observational quantities in the equation are small in practice for a source such as GX 5-1, the estimate of the spin frequency in such a source is largely dictated by the estimate of ξ. This is illustrated in Figure 2, which shows allowable regions in ν_s, ξ space for GX 5-1. For values of ν_s and ξ within the shaded region, an acceptable fit (which we define as ν_Q, determined from eq.(21), being within 1 Hz of the observed ν_Q) of eq.(21) to the data for GX5-1 can be obtained.

ξ can be derived from the magnetospheric model presented above. The general result is algebraically complicated and not directly very enlightening. In order to illustrate the dependence of ξ on parameters such as ω_s and $\Lambda_\mu = -(R_m/\mu_{eff})d\mu_{eff}/dR_m$, in Table (2) we present analytic expressions for ξ for two sets of simple limiting cases.

Since we expect Λ_μ to be positive [e.g., from eq. (19), $\Lambda_\mu = (\mu_{eff}/\mu - 1) \approx (1 - R_s/R_m)^{-1} - 1$], the enhancement of the magnetic field within the magnetosphere by screening currents flowing within the disk tends to "stiffen" the magnetosphere (i.e. lower the value of ξ for a wide range of parameters. For low ξ, R_m responds with relative insensitivity to variations in mass accretion rate.) If neutron stars in LMXB Z sources are rotating as fast as the fastest observed radio pulsars (641 Hz), then Λ_μ could be as large as 2.4. This would require a "stiff" neutron star equation-of-state. For a relatively "soft" eos, $\Lambda_\mu \sim 1.4$.

In all cases except (d) in Table (2), ξ either does not depend on ω_s or is lowered for increasing values of ω_s. Except for (c) and (e), all cases allow low values of ξ. A stiff magnetosphere gives good fits to data from GX5-1, for comparatively high stellar spin frequencies. For example, with a stellar spin period near that of the fastest radio millisecond pulsars (1.5 ms), the GX5-1 HBO requires $\xi \sim 0.075$.

Given a value of ξ (i.e., an assumed spin frequency), the QPO observations and the magnetospheric model constrain the neutron star magnetic moment μ. Table (3) shows the values of μ derived for the limiting cases shown in Table (2), assuming $\nu_s = 641$ Hz and $\xi = 0.075$.

Since we expect $(\lambda/\zeta) \geq 1$, $\alpha < 1$, and $\Lambda_\mu \geq 1$, we conclude that the model yields magnetic field strengths in a range consistent with those inferred from observed spin-down rates in the fastest millisecond radio pulsars ($\mu_{27} \sim 0.1 - 0.6$) (Camilo, Thorsett & Kulkarni 1994).

In Figure 3 we show a fit (solid line) of eq. (21), with $\nu_s = 641$ Hz and $\xi \approx 0.075$, to the HB QPO of GX5-1. Also shown (dashed line) is a fit of eq. (1) to the data, directly using eq.(13) to determine R_m rather than resorting to the power law (ξ = constant) approximation used above. We have assumed $\beta_\gamma = 1$, $\beta_v = 1$, and $\Lambda_\mu = 1$. Acceptable fits can be obtained for a relatively broad range of parameters representing cases intermediate between (a) and (e) in Table (2).

We can also use eqs. (18) and (22) to directly calculate the effective magnetic moment. For the case where $\beta_m = 1, \beta_v = 1, \beta_\gamma = 1$, we find

$$\mu^2_{eff27}(R_m) = 6.8\times10^4 \frac{m^2 L_{x/e}}{(\nu_s+\nu_Q)^{7/3}}\left[2.0\alpha m^{2/3}+1.2\left(\frac{\zeta}{\lambda}\right)^{1/2}\left(\frac{\mu_{eff27}(R_m)}{\nu_Q}\right)^{1/2}\left(\frac{\alpha}{m^2 L_{x/e}}\right)^{1/4}(\nu_s+\nu_Q)^{3/4}\right] \tag{25}$$

where $L_{x/e} = L_x/L_{edd}$ is the luminosity in units of the eddington luminosity. If we let $\beta_\gamma = 0$ while keeping $\beta_m = 1, \beta_v = 1$ then we obtain

$$\mu^2_{eff27}(R_m) = 6.8 \times 10^4 \frac{m^2 L_{x/e}}{(\nu_s+\nu_Q)^{7/3}}\left[2.0\alpha m^{2/3} + \frac{500}{(\nu_s+\nu_Q)^{2/3}}\right] \tag{26}$$

Since these two equations are for the effective magnetic dipole moment, we expect the intrinsic dipole moment to be somewhat less than this. If we adopt the form given by eq. (19), we expect $\mu \approx \mu_{eff}(1 - 6.7 \times 10^{-3}(\nu_s + \nu_Q)^{2/3})$ (assuming $R_s = 10^6$cm). In Figure 4 we plot eqs. (25) and (26) assuming $\alpha = 0.1$, $(\lambda/\zeta) = 1$, $m = 1.4$, $\nu_Q = 36Hz$ and $L_{x/e} = 1$, with and without the correction for magnetic screening. We have also plotted several known magnetic dipole moments of millisecond pulsars versus their spin frequency (Camilo, Thorsett & Kulkarni 1994).

5. Discussion

The model presented here represents an alternative picture of the HB within a broader synthesis of Z source behavior such as that of Lamb (1989). We have not attempted to treat the other branches of the Z diagram because it is clear that a different mechanism is responsible for QPO oscillations on these branches. The central issue under investigation has been the relationship between ν_s and ξ, represented in Figure 2, and the constraints that HB QPO place on these parameters. We note the following considerations favoring our modified beat frequency model: (i) incorporation of relevant physical effects such as radiation pressure; (ii) consistent treatment of the effects of stellar spin in determining the accretion torque and the magnetosphere radius; (iii) preservation of the fit of the model to the observed luminosity dependent QPO frequency; and (iv) agreement of stellar spin

periods and magnetic moments determined by fits to the model with those observed for the fastest radio pulsars. The central conclusion we reach is that ν_s in Z sources is at least $\sim$ 400 Hz and that values as high as observed in the fastest millisecond radio pulsars (641 Hz) are consistent with observation and magnetosphere theory.

Recent observations of Sco X-1 and (van der Klis et al. 1996) 4U1728-34 (Strohmayer, Zhang, and Swank 1996) with XTE have revealed $\sim$ 1000 Hz and $\sim$ 800 Hz QPO respectively, which may represent the Keplerian frequency of the inner edge of the disk. Although Sco X-1 has not been observed on the Horizontal Branch, and therefore has no measured HB QPO, if we assume that $\omega_s \sim \omega_{sc} \sim 1$ then the spin frequency would also be $\sim$ 1000 Hz. Noting that $\nu_K = \nu_s + \nu_Q$ in our model, we can estimate the surface magnetic field $B \sim 1 - 3 \times 10^8$ G, consistent with the millisecond pulsars. The question which still has to be answered is why the coherent pulse period has not yet been seen, while the inner edge of the disk has been seen. One possible explanation is that a weak pulse from the neutron star surface would be strongly attenuated by gravitational lensing as discussed in section 2, while the QPO from the disk at a distance of several stellar radii would be essentially unaffected. This weak pulsar signal could then be obscured by the broad ($\sim$ 50 Hz FWHM) disk QPO. Further analysis of the data may yet reveal an underlying coherent signal.

In a subsequent paper, we will consider further the robustness of the foregoing model. For the present, we will simply mention some of the observational and theoretical considerations that support the revised model which will be discussed in detail later. First, the width of the QPO features and their variation of intensity is a natural result of the model. Observations of HB QPO from GX 17+2 have suggested that the dominant mechanism contributing to the width of the QPO is smearing in ν_Q due to repeated interaction of accreting clumps with stellar magnetic field as the clumps drift inward across a transition zone of finite radial extent (Penninx et al. 1990). The above expression for R_m implies a spectral width more consistent with observations of GX5-1 (van der Klis et al. 1985) than that derived from the conventional BFMA model. Secondly, the relationship between QPO frequency and the evolution of the neutron star's magnetic field derived from the model is consistent with the observed dispersion in the magnetic fields inferred in the fastest millisecond radio pulsars and the $\delta < \nu_Q > / < \nu_Q >$ observed in Z-sources.

A possible argument against the model is the high shot rate required for the implicit correlation between the QPO and the low frequency noise component of the Fourier power spectrum. Lack of detection of such a correlation in GX5-1 requires a shot rate greater than 400Hz, which has been claimed to be inconsistent with the BFMA model (Norris et al. 1990). However, that calculation, which implied a maximium shot rate of 300 Hz, assumed no

variance in the shot amplitude. However, if there is a *distribution* of shot amplitudes, such as an exponential distribution, the limit of the shot rate becomes 600 Hz, consistent with observation. Another possible problem is the onset of the Chandrasekhar-Friedman-Schutz (CFS) gravitational radiation reaction instabilility when the neutron star is spun up to the frequencies ($\nu_s \geq 640$Hz) implied by the model. However, a calculation by Meidell and Lindblom (1991) suggests that if the neutron star is below 10^9 K and in a superconducting state, then the viscosity due to electron scattering from superfluid vortices will suppress the CFS instability.

6. SUMMARY

We have presented a new model of horizontal branch QPOs that is based on the beat frequency modulated accretion model. Its departures from the original BFMA model correct recognized deficiencies. The model predicts high stellar spin frequencies ($>$ 400 Hz) that fall in a range where pulsation upper limits pose no problem. The magnetic field and spin frequency range are also compatible with those of the fastest radio pulsars. However, detection of the stellar spin period is the only hope of rigorous confirmation. Short of that, the model presented comes close to incorporating all available information.

The authors acknowledge helpful discussions with R.V. Wagoner, M. Nowak, B. Vaughan, and P. Hertz. We also thank N. Shibazaki for several illuminating discussions about QPOs and for pointing out to us the work of Wang. KSW acknowledges support from the Office of Naval Research. PFM and MSER acknowledge support from Stanford University.

A. Accretion Torque and the Critical Fastness Parameter

Assuming the magnetic field pitch distribution γ_ϕ given by eq.(8) and a thin, gas- pressure dominated disk, Wang (1987) calculated the accretion torque and found $\omega_{sc} = 0.941$, where ω_{sc} is the critical fastness parameter for which the accretion torque vanishes (Ghosh & Lamb 1979). In the GL model, $\omega_{sc} = 0.35$.

Observations of QPO in the x-ray pulsars Cen X-3 (Tennant 1988, Takeshima et al. 1991), EXO 2030+375 (Angelini, Stella and Parmar 1989) and X1627-673 (Shinoda et al. 1990) provide important observational tests of both the beat frequency model of QPOs and of accretion torque models (Shibazaki 1989). We note again that observations in these

systems are not necessarily directly relevant to the QPO observed in LMXBs, but at least provide supporting evidence for some of the key assumptions made in modelling the HB QPOs in the LMXB Z sources.

Table (A1) lists the observed spin frequencies, QPO frequencies and spin period derivatives for each of the above sources. Also listed are the values of the fastness parameter derived by assuming the beat frequency relation of eq.(1) is valid. For Cen X-3 and X1627-673 the fastness parameter is much larger than the critical fastness of GL but below that of Wang. Both of these sources are observed to be spinning-up, consistent with the Wang model but not with the GL model. For EXO 2030+375, the fastness parameter is below the critical value for both the GL model and the Wang model.

In the Wang theory, the period derivative is given by

$$-\dot{P}/P = 4.28\times10^{-5} f(\omega_s)\left(\frac{P}{1s}\right)^{4/3}\left(\frac{L_x}{10^{37}\mathrm{ergs}^{-1}}\right)\left(\frac{1.4M_\odot}{M}\right)^{4/3}\left(\frac{10^6\mathrm{cm}}{R_s}\right)\mathrm{yr}^{-1} \quad \text{(A1)}$$

$$f(\omega_s) = \omega_s^{1/3} + \frac{2}{9}\omega_s^{31/120}\left[1-\omega_s-\frac{\omega_s^{3/2}}{(1-\omega_s)^{1/2}}\right] \quad \text{(A2)}$$

For parameters derived from observation and the beat frequency relation, eq(A1) can be used to calculate $(\dot{P}/P)$, which can then be compared with the observed value. The theoretical values are shown in the last column of Table (A1). Given the uncertainties in determining the luminosity (distance) and uncertainties in the masses and radii of the neutron stars in these systems, the agreement of observation with theory is satisfactory. In the case of Cen X-3 the theoretical value of $\dot{P}$ differs from observation by a substantial amount. However in this source $\dot{P}$ shows considerable fluctuations about the mean value shown in the Table (A1). We also note that Parmar et al. (1989) analyzed an EXOSAT observation of EXO 2030+375 during an x-ray outburst in which the luminosity changed by more than 10^3. They found that $-\dot{P} \propto L^{1.16\pm0.12}$. This is also in reasonable agreement with the luminosity dependence expected from eq.(A1), namely $-\dot{P} \propto L^{1.0}$. The GL theory predicts $-\dot{P} \propto L^{0.86}$. Similarly, Wilson et al. (1993) have found that for GS0834-430 $-\dot{P} \propto L^{0.924\pm0.085}$.

In the remainder of this appendix we evaluate the accretion torque and ω_{sc} in the limit of a radiation pressure dominated inner disk. Following GL and Wang, the accretion torque is given by

$$N = \dot{M}(GMR_m)^{1/2} + \int_{R_m}^{R_c}|B_\phi|B_z r^2 dr - \int_{R_c}^{R_o}|B_\phi|B_z r^2 dr \quad \text{(A3)}$$

where $R_c = (GM/\Omega_s^2)^{1/3}$ is the corotation radius and R_o is either the outer radius of the disk or $\sim$ the light-cylinder radius. Magnetic field penetrating the disk for $r > R_c$ provides

a spin-down torque, while field between R_m and R_c enhances the spin-up torque. As first shown by GL, the spin-down contribution to the torque can equal or exceed the spin-up contributions.

The spin-down contribution to N can be written as

$$N_- = -\int_{R_c}^{R_o} \gamma_\phi(r) B_z^2 r^2 dr \tag{A4}$$

or, using eq.(8),

$$N_- = -(\xi/\zeta)^{1/2} \int_{R_c}^{R_o} [(r/R_c)^{3/2} - 1]^{1/2} [(\dot{M}/r)(h/r)(v_K/v_r)\Omega_K]^{1/4} B_z^{3/2} r^2 dr \tag{A5}$$

For a RPD disk we assume

$$(h/r)(v_K/v_r) = (1.4/\alpha c) R_g^{-3/2} (GM)^{1/2} r \tag{A6}$$

Substituting eq.(A6) into (A5) and assuming $B_z = \mu/r^3$,

$$N_- = -\frac{2}{3} N_c \int_r^{y_o} (y-1)^{1/2} y^{-23/12} dy \tag{A7}$$

where

$$N_c = (\xi/\zeta)^{1/2} [(1.4/\alpha c) GM\dot{M} R_g^{-3/2}]^{1/4} \mu^{3/2} r_c^{-15/8} \tag{A8}$$

The integration variable $y = (r/R_c)^{3/2}$ and $y_o = (R_o/R_c)^{3/2}$. The spin-up torque can be written in a similar form;

$$N_+ = \dot{M}(GMR_m)^{1/2} + \frac{2}{3} N_c \int_{\omega_s}^{1} (1-y)^{1/2} y^{-23/12} dy \tag{A9}$$

noting that $\omega_s = (R_m/R_c)^{3/2}$.

Now define $N_o^2 = \dot{M}^2 GMR_m$. It can be shown that

$$N_o^2 = 4N_c^2 (1-\omega_s)\omega_s^{-5/2} (\delta/R_m)^2 [\delta/R_m + 2\tilde{\beta}_m(1-\omega_s)]^{-2} \tag{A10}$$

Following GL, it is convenient to introduce the dimensionless accretion torque $\eta(\omega_s)$ defined by

$$N = N_o \eta(\omega_s) \tag{A11}$$

If we approximate $y^{-23/12}$ as y^{-2}, then the integrals in eq.(A7) and eq.(A9) can be done analytically with the result that

$$\eta(\omega_s) = 1 + \frac{1}{3}[1 + \Gamma(1-\omega_s)^{1/2}][\omega_s^{1/4} + \frac{\omega_s^{5/4}(\tanh^{-1}(1-\omega_s)^{1/2} - (\tan^{-1}(y_o-1)^{1/2} - \frac{(y_o-1)^{1/2}}{y_o}))}{(1-\omega_s)^{1/2}}] \tag{A12}$$

where $\Gamma = 2\tilde{\beta}_m(\xi/\zeta)^{1/2}[(h/R_m)(v_K/v_r)]^{-3/4}[(\dot{M}/R_m)\Omega_K]^{1/4}B_z^{-1/2}$. Note that Γ does not explicitly depend on the stellar spin frequency. It does depend on R_m.

The Wang magnetosphere radius criteria corresponds to the limit $\Gamma = 0$. To determine the critical fastness parameter ω_{sc} for which $\eta = 0$, Wang also assumed $y_o = \infty$ and a gas pressure dominated disk. He found $\omega_{sc} = 0.94$. Evaluating eq.(A12) for $\Gamma = 0$ and $y_o = \infty$ gives

$$\eta(\omega_s) = 1 - (\pi/6)(1-\omega_s)^{-1/2}\omega_s^{5/4} + \frac{1}{3}\omega_s^{1/4} + \frac{1}{3}\omega_s^{5/4}(1-\omega_s)^{-1/2}\tanh^{-1}((1-\omega_s)^{1/2}) \quad \text{(A13)}$$

This function is shown as the $\Gamma = 0$ curve in Figure (A1). For $\omega_s = 0.918$, the accretion torque vanishes. This value is slightly less than the critical fastness for a gas pressure dominated disk. The other curves in Fig.(A1) show the behavior of $\eta(\omega_s)$ for fixed values of Γ. For parameters appropriate to RPD disks and typical LMXB Z sources, we expect $\Gamma \leq 10$. As Γ increases from zero the critical fastness parameter decreases but always satisfies the condition $\omega_{sc} \geq 0.65$.

For a very rapidly spinning neutron star, the light cylinder radius, $R_{lc} = c/\Omega_s = 74.45\text{km}(640\text{Hz}/\nu_s)$, may only be a few times the corotation radius R_c since

$$R_{lc}/R_c = (c^3/(GM\Omega_s^2))^{1/3} = 3.2(640\text{Hz}/\nu_s)^{2/3}(1.5M_\odot/M)^{1/3} \quad \text{(A14)}$$

In this case letting $y_o \rightarrow \infty$ is not the appropriate limit and, in any case, the integrand in eq.(A7) becomes a poor approximation when r approaches or goes beyond R_{lc}. Lacking a theory valid in this regime, we resort to approximating the effects of rapid rotation by taking the upper limit of integration in eq.(A12) as

$$y_o = (R_{lc}/R_c)^{3/2} = \omega_s^{-1/2}(GM/R_m c^2)^{-3/4} \quad \text{(A15)}$$

The curves in Figure (A2) show $\eta(\omega_s)$ for various values of Γ assuming relation (A14). The main effect of introducing this cutoff is to increase ω_{sc}. For $\Gamma = 0$, $\omega_{sc} = 0.978$. As Γ increases, ω_{sc} decreases but satisfys the inequality $\omega_{sc} \geq 0.88$.

Figure (A3) is a contour plot illustrating the dependence of η on ω_s and Γ for two limiting cases; (a) $y_o = \infty$ and (b) $y_o = (R_{lc}/R_c)^{3/2}$. In both cases $\eta = 1$ for $\omega_s = 0$. [1]

---

[1]Recall that we approximated $y^{23/12}$ by y^2. This approximation breaks down for $\omega_s = 0$. If this approximation is not made, the value of η is slightly greater than 1 for $\omega_s = 0$. In evaluating the torque in the gas pressure dominated case, Wang (1987) makes a similar approximation; $y^{291/120} \sim y^{5/2}$. In this case, the approximation leads to a divergence of η for $\omega_s = 0$. If the approximation is not made then η is well behaved for $\omega_s = 0$. Ghosh and Lamb (1991) have criticized Wang's torque theory because of the presence of this divergence. This criticism is not valid.

Table 1. Limits on pulse fractions in Z sources for spin frequencies up to 500 Hz.[a]

Source	pulse fraction
Sco X-1	$< 0.57\%$
GX 340+0	$< 1.8\%$
GX 17+2	$< 1.6\%$
Cyg X-2	$< 1.4\%$
GX 5-1	$< 0.99\%$
GX 349+2	$< 1.3\%$

[a]99% confidence Vaughan et al. 1994.

Table 2. The exponent ξ for several limiting cases indicated by the values of the parameters in the first column.

parameter values	ξ	range of ξ
$\tilde{\beta}_m(1-\omega_s) << 1/2\delta/R_m$		
(a) $\beta_\gamma = 1; \beta_v = 1$	$3/7(1+4/7\Lambda_\mu + 2/7\omega_s/(1-\omega_s))^{-1}$	$0 \leq \xi \leq 0.102$
(b) $\beta_\gamma = 1; \beta_v = 0$	$3/10(1+8/15\Lambda_\mu + 3/15\omega_s/(1-\omega_s) + 1/20\omega_s/(1+\omega_s))^{-1}$	$0 \leq \xi \leq 0.092$
(c) $\beta_\gamma = 0; \beta_v = 0, 1$	$3/7(1+4/7\Lambda_\mu)^{-1}$	$0.429 \geq \xi \geq 0.181$
$\tilde{\beta}_m(1-\omega_s) >> 1/2\delta/R_m$		
(d) $\beta_\gamma = 1, 0; \beta_v = 0$	$3/25(1+12/25\Lambda_\mu - 6/25\omega_s/(1-\omega_s) + 3/25\omega_s/(1+\omega_s))^{-1}$	$\xi \geq -0.071$
(e) $\beta_\gamma = 1, 0; \beta_v = 1$	$3/5(1+4/5\Lambda_\mu)^{-1}$	$0.205 \leq \xi \leq 0.60$

Table 3. Neutron star magnetic moment for various cases defined in Table (1), assuming that $\nu_s = 641$ Hz and $\xi = 0.075$.

Case	μ_{27}
(a)	$6.35(\lambda/\zeta)^{-1/3}\alpha^{1/6}(\Lambda_\mu + 1)^{-1}$
(b)	$0.744(\lambda/\zeta)^{-3/8}(\Lambda_\mu + 1)^{-1}$
(d)	$0.233\tilde{\beta}_m^{1/6}(\Lambda_\mu + 1)^{-1}$

Table A1. QPO properties of x-ray pulsars. Shown in the table are the observed spin and QPO frequencies, the fastness parameter (assuming the beat frequency relation), the observed spin period derivative, and the theoretical spin period derivative calculated using eq.(A1). Parameters in the first three columns are summarized in Shibazaki (1989).

Pulsar	ν_s (Hz)	ν_Q (Hz)	ω_s	$(\dot{P}/P)_{obs}(\mathrm{yr}^{-1})$	$(\dot{P}/P)_{theory}(\mathrm{yr}^{-1})$
SMC X-1	1.410	0.010	0.993		$+2.2 - +2.6 \times 10^{-3}$
4U0115+63	0.277	0.062	0.817		-4.3×10^{-4}
V0332+53	0.229	0.051	0.818		-5.7×10^{-4}
Cen X-3[a]	0.207	0.035	0.855	-3×10^{-4}	-1.9×10^{-3}–
					-0.6×10^{-4}
X1627-673[b]	0.131	0.04	0.76	-2.2×10^{-4}	-4.8×10^{-4}
EXO 2030+375[c]	0.0239	0.21	0.10	-3×10^{-2}	-6×10^{-2}
A0535+26	0.0096				

[a]The maximum (minimum) x-ray luminosity is $8 \times 10^{37}(2.6 \times 10^{36})$erg s^{-1} for an assumed distance of 10 kpc (Bradt & McClintock 1983). $(\dot{P}/P)_{obs}$ shows considerable fluctuations with time about the value shown (Nagase 1989). The range shown for $(\dot{P}/P)_{theory}$ corresponds to the range of observed luminosity.

[b]The x-ray luminosity is 10^{37}erg s^{-1} for an assumed distance of 8 kpc (Shinoda et al. 1990). $(\dot{P}/P)_{obs}$ is relatively steady in this source (Nagase 1989).

[c]$(\dot{P}/P)_{obs}$ is from Parmar et al. (1989) for a luminosity of 9×10^{37}erg s^{-1}, assuming a distance of 5 kpc.

· In all cases the neutron star mass and radius are assumed to be $1.4M_\odot$ and 10^6 cm, respectively.

REFERENCES

Alpar, M., & Shaham, J. 1985, Nature, 316, 239

Angelini, L., Stella, L., & Parmar, A. N. 1989, Ap. J., 346, 906

Asaoka, I. & Hoshi, R. 1989, Pub. Astr. Soc. Japan, 41, 1049

Bhattacharya, D., & van den Heuvel, E.P.J. 1991, Phys. Rep., 203, 1

Bradt, H.V.D. & McClintock, J.A. 1983, Ann. Rev. Astron. Astrophys. 21, 13

Brainerd, J. & Lamb, F.K. 1987, Ap. J., 317, L33

Bussard, R.W., Weisskopf, M.C., Elsner, R.F., & Shibazaki, N. 1988, Ap. J., 327, 284

Camilo, F., Thorsett, S.E., & Kulkarni, S.R. 1994, Ap. J. Lett., 421, L15

Chandrasekhar, S., 1970, Phys. Rev. Letters, 24, 611

Chen, K. & Shaham, J. 1989, Ap. J., 339, 279

Friedman, J.L., Ipser, J.R., & Parker, L. 1986, Ap. J., 304, 115

Friedman, J.L., & Schutz, B.F. 1978, Ap. J., 222, 281

Ghosh, P., & Lamb, F.K. 1979, Ap. J., 234, 296

Ghosh. P., & Lamb, F.K. 1991, to appear in Neutron Stars, ed. J. Ventura (Kluwer Academic, in press)

Hasinger, G. 1986, in The Origin and Evolution of Neutron Stars (Nanjing, China; 1986 May 26-30), ed. D.J. Helfand & J.H. Huang (Dordrecht: Reidel)

Hasinger, G., & van der Klis, M. 1989, Astron. Astrophys., 225, 79.

Helfand, D., Ruderman, M., & Shaham, M.A. 1983, Nature, 304, 423

Hertz, P., Norris, J.P., Wood, K.S., Vaughan, B.A., & Michelson, P.F. 1990, Ap. J., 354, 267

Hirano, T., Hayakawa, S., Kunieda, H., Makino, F., Masai, K., Nagase, F., & Yamashita, K. 1984, Pub.Astr.Soc.Japan, 36, 169

Joss, P., & Rappaport, S. 1983, ApJ, 270, L73

Lamb, F.K., Shibazaki, N., Shaham, J., & Alpar, M.A. 1985, Nature, 317, 681

Lamb, F.K. 1989, in Proc. 23rd ESLAB Symp.: Two Topics in X-ray Astronomy, ed. J. Hunt & B. Battrick (Noordwijk: ESA), 1, 215

Lewin, W.H.G., Van Paradijs, J., & Van der Klis, M. 1988, Space Sci.Rev., 46, 273

Lindblom. L., and Detweiler, S.L. 1977, ApJ, 211, 565

Meidell, G. & Lindblom, L. 1991, Annals of Physics, 205, 110

Mitsuda, K., Dotani, T., Yoshida, A., Vaughan, B.A., & Norris, J.P. 1991, Pub.Astr.Soc.Japan, 43, 113

Mitsuda, K., Dotani, T. 1989, Pub.Astr. Soc. Japan 41, 557

Nagase, F. 1989, Publ. Astr.Soc. Japan 41, 1

Narayan, R. & Popham, R. 1989, Ap. J., 346, L25

Norris, J., et al. 1990, Ap. J., 361,514

Parker, E. N. 1955, Ap. J., 121, 491

Parmar, A.N., et al. 1989, Ap.J., 338, 359

Paczynski, B. 1983, Nature, 304, 421

Penninx, W., et al. 1990, MNRAS, 243, 114

Popham, R. & Narayan, R. 1991, Ap. J. 370

Roberts, P.H., & Stewartson, K. 1963, ApJ, 137, 777

Ruderman, M. 1991, Ap. J., 382, 576

Ruderman, M. 1991b, Ap. J., 382, 587

Savonije, G. J. 1983, Nature, 304, 422

Shakura, N.I., & Sunyaev, R.A. 1973, Astron. Astrophys., 24, 337

Shibazaki, N. & Mitsuda, K. 1984, in High Energy Transients in Astrophysics, ed. S.E. Woosley (New York: AIP), p. 63

Shibazaki, 1989, in Proc. 23rd ESLAB Symp.: Two Topics in X-ray Astronomy, ed. J. Hunt & B. Battrick (Noordwijk: ESA), 1, 215.

Shinoda, K., Kii, T., Mitsuda, K. Nagase, F., Tanaka, Y., Makishima, K., & Shibazaki, N. 1990, Pub. Astr. Soc. Japan, 42, L27

Schulz, N.S. & Wijers, R.A.M.J. 1993, A.&A., 273, 123

Strohmayer, T., Zhang, W. & Swank, J. 1996, IAUC 6320

Takeshima, T. Dotani, T., Mitsuda, K. & Nagase, F. 1991, Pub. Astr. Soc. Japan, 43, L43

Tennant, A. 1988, a talk presented at The Fifth Los Alamos Space Physics/Astrophysics Workshop "Quasiperiodic Oscillations in Luminous Galactic X-Ray Sources," La Cienega, NM, October 1988

Treves, A., Maraschi, L., Abramowicz, M. 1988, Pub. Astro. Soc. Pac., 100, 427

van den Heuvel, E.P.J. 1977, Ann. N. Y. Acad. Sci., 302, 14

van der Klis, M., et al. 1985, Nature, 316, 225

van der Klis, M., et al. 1996, IAUC 6319

van der Klis, M. 1989. Ann. Rev. Astron. Astrophys., 27, 517

Vaughan, B. A., et al. 1994, Ap. J. 435, 362

Wagoner, R.V. 1984, Ap. J. 278, 395

Wang, Y.-M. 1987, Astron.Astrophys., 183, 257

Wang, Y.-M. 1995, Ap. J. Lett. 449, L153

Weisskopf, V. 1975, Science, 187, 605

White, N., & Holt, S. 1982, ApJ, 257, 318

White, N. & Stella, L. 1988, MNRAS, 231, 325

Wood, K.S., Ftaclas, C., & Kearney, M.W., 1988, Ap. J. Lett., 324, L63

Wood, K.S., et al. 1991, Astrophys. J. , 379, 295

Fig. 1.— Comparison of pulsation upper limits for various LMXB sources (solid curves labeled Sco X-1 and GX5-1; other LMXB limits mentioned in the text lie between these two sources) with attenuation expected from scattering in a hot corona surrounding the source (dashed curves). The coronal attenuation depends on R_c and τ. At low frequencies the attenuation (the parameter $R_c\tau$) is constrained by the observed QPO power (cross-hatched region). At high frequencies the attenuation approaches $e^{-2\tau}$. From observed temporal lags and spectral fits to coronal models, the Thompson depth is likely to be in the range from 4 to 7.

Fig. 2.— Allowable regions in ν_s, ξ space that give acceptable fits to the frequency dependent QPO observed in GX 5-1.

Fig. 3.— Comparison of a fit (solid curve) of eq.(21), with $\nu_s = 641$ Hz and $\xi = 0.075$, to the HB QPO observed in GX 5-1. The dashed curve is a fit of eq.(1) to the data, directly using the magnetosphere radius relation, eq.(16), with $\beta_\gamma = 1$, $\beta_v = 1$, and $\Lambda_\mu = 1$.

Fig. 4.— Magnetic dipole moment as a function of spin frequency from eqs. (25) (solid curve) and (26) (dashed curve) assuming a QPO frequency of 36 Hz, viscosity parameter $\alpha = 0.1$, neutron star mass of $1.4M_\odot$, and Eddington luminosity. If we correct for magnetic screening, we obtain the short dashed (25) and dotted (26) curves. Also plotted are the intrinsic magnetic moments for the fastest millisecond pulsars (dots)(Camilo, Thorsett & Kulkarni 1994).

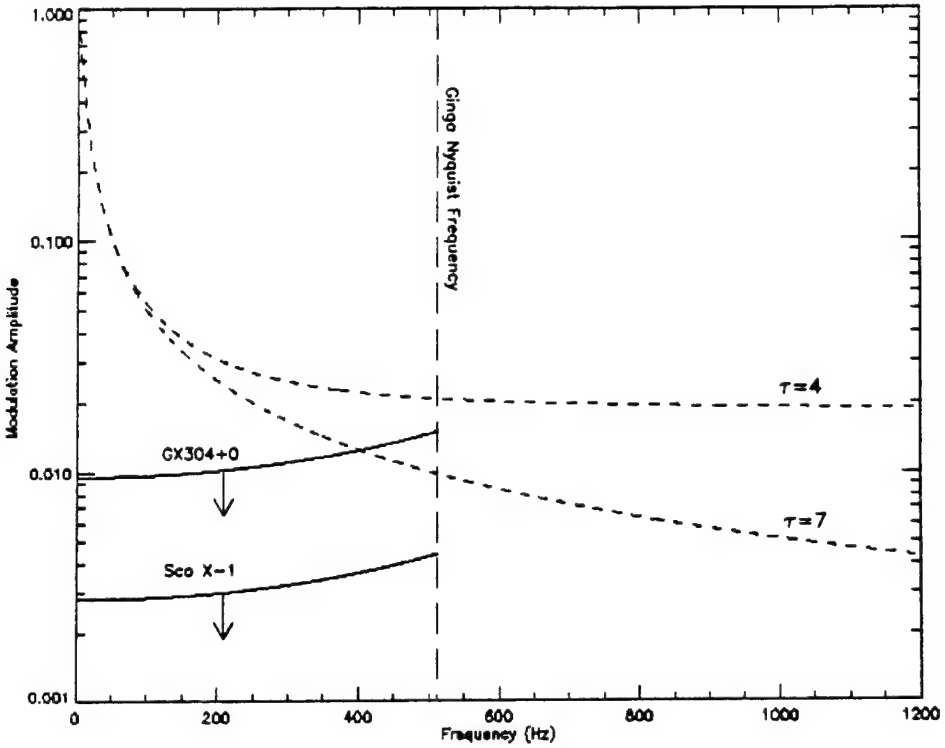
1.000
0.100
0.010
0.001
Modulation Amplitude
0
200
400
600
800
1000
1200
Frequency (Hz)
Ginga Nyquist Frequency
τ=4
τ=7
GX304+0
Sco X-1

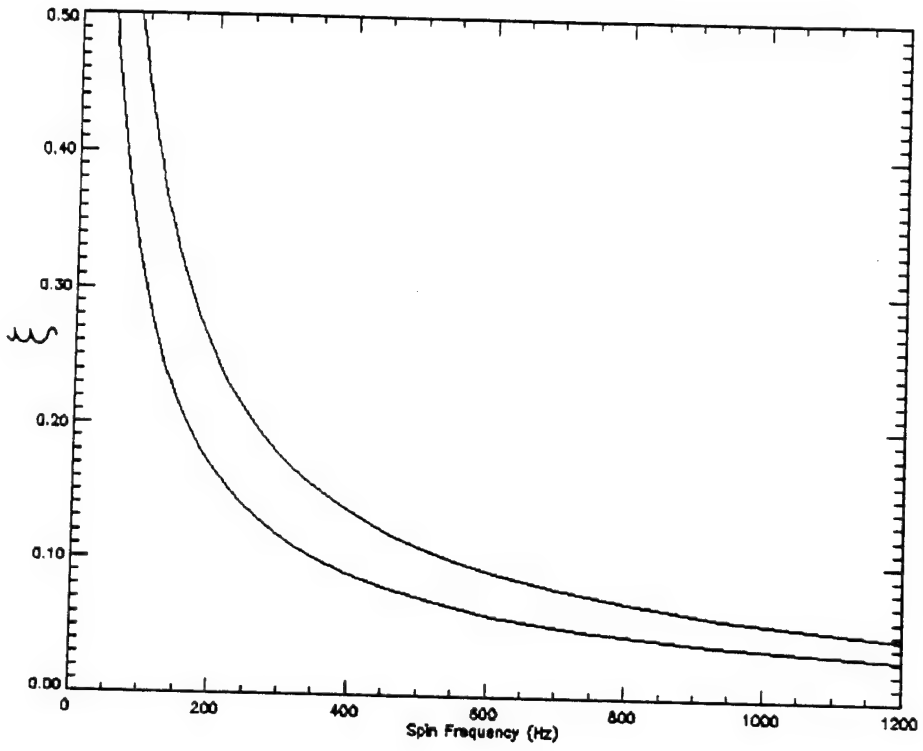
0.50
0.40
0.30
0.20
0.10
0.00
0
200
400
600
800
1000
1200
Spin Frequency (Hz)

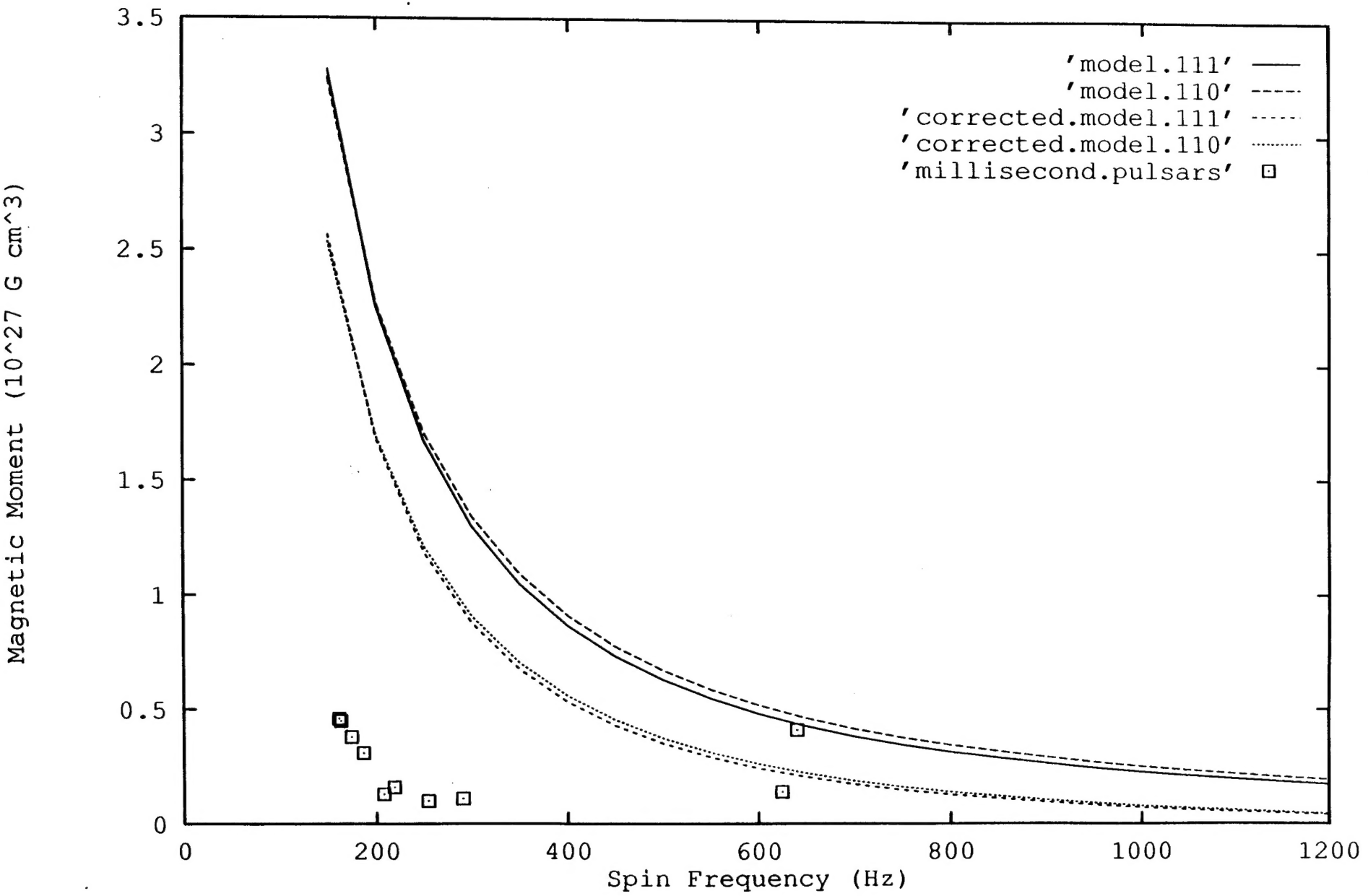
'model.111'
'model.110'
'corrected.model.111'
'corrected.model.110'
'millisecond.pulsars'
Magnetic Moment (10^27 G cm^3)
Spin Frequency (Hz)
0
0.5
1
1.5
2
2.5
3
3.5
0
200
400
600
800
1000
1200

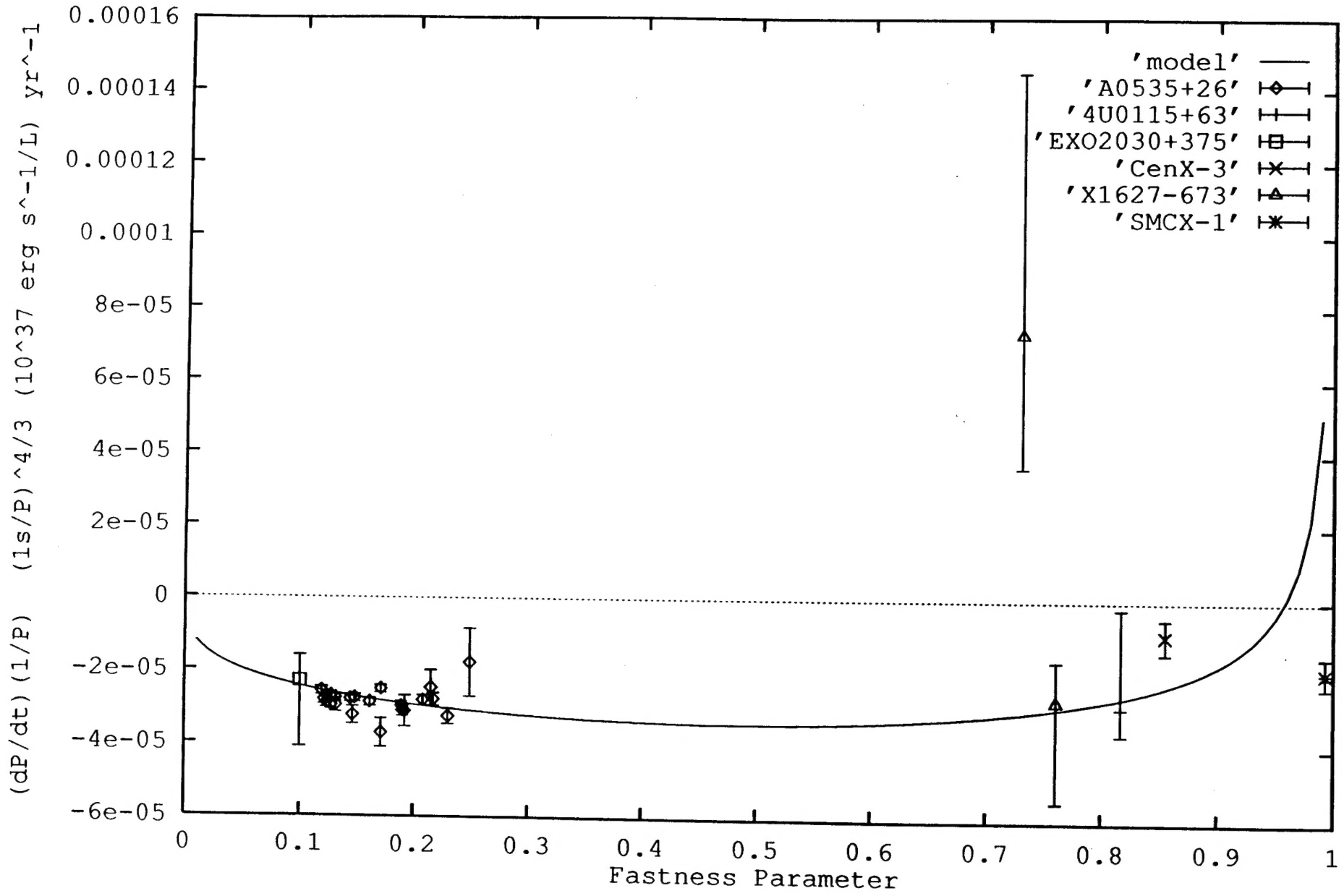
'model'
'A0535+26'
'4U0115+63'
'EXO2030+375'
'CenX-3'
'X1627-673'
'SMCX-1'
(dP/dt)(1/P) (1s/P)^4/3 (10^37 erg s^-1/L) yr^-1
0.00016
0.00014
0.00012
0.0001
8e-05
6e-05
4e-05
2e-05
0
-2e-05
-4e-05
-6e-05
0
0.1
0.2
0.3
0.4
0.5
0.6
0.7
0.8
0.9
1
Fastness Parameter

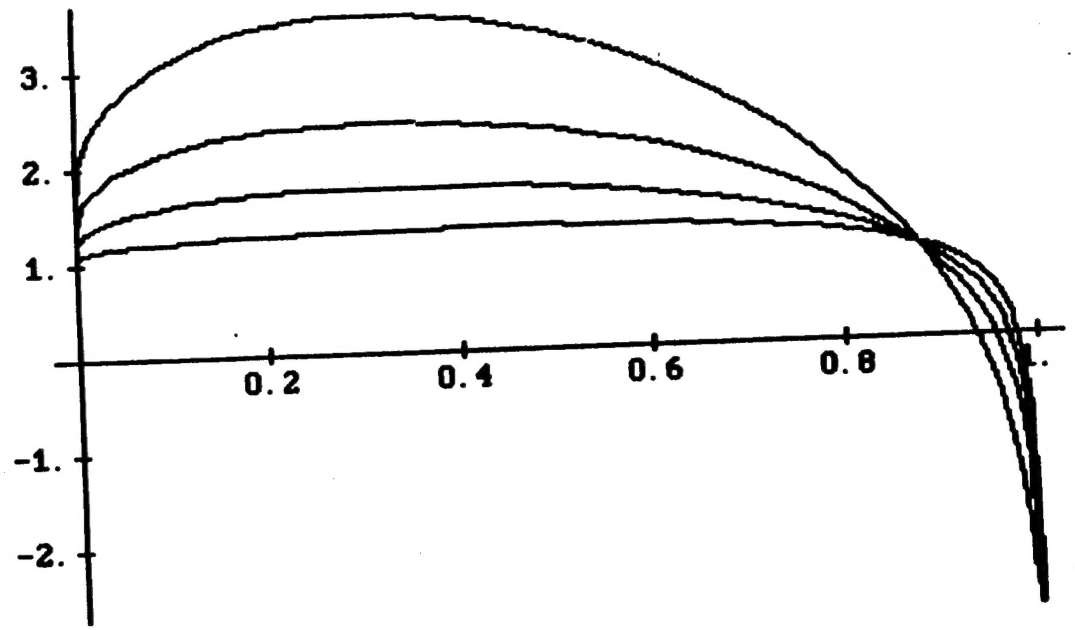

Figure A2. Dimensionless torque as a function of the fastness parameter ws. The torque is computed for a radiation dominated magnetosphere using the model of Wang (1987). The upper limit of integration of the integral that determines the spin-down contribution to the torque [see eq. (A4)] is set equal to the light-cylinder radius.

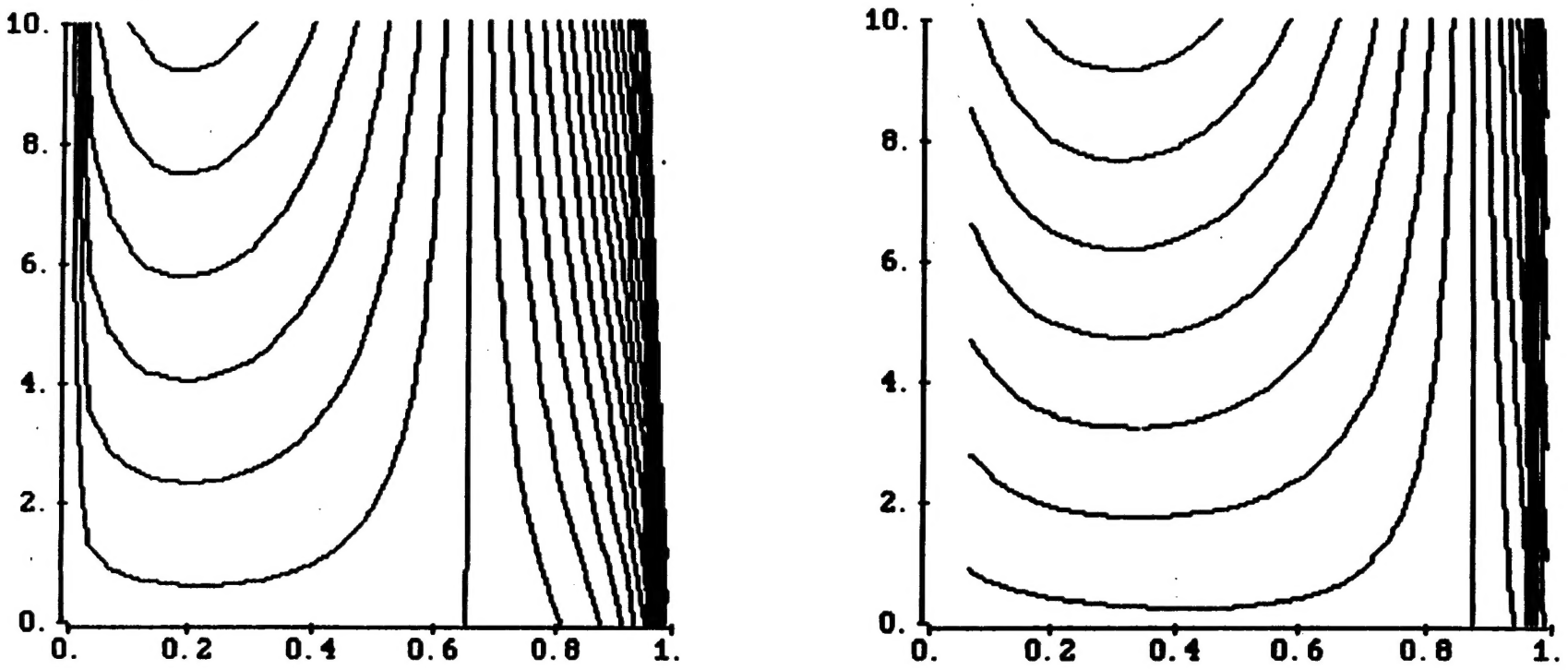

Figure (A3). Contour plots of dimensionless torque η, illustrating the dependence on Γ and α_s. For case (a), $y_0 = \infty$, while for case (b), $y_0 = (R_{lc}/R_c)^{3/2}$.